Kinetic Properties of a MNB/DYRK1A Mutant Suitable for the Elucidation of Biochemical Pathways†

Tatyana Adayev,‡ Mo-Chou Chen-Hwang,‡ Noriko Murakami,‡ Jerzy Wegiel,§ and Yu-Wen Hwang*,‡

Molecular Biology Department and Develomental Neurobiology Department, New York State Institute for Basic Research in Developmental Disabilities, Staten Island, New York 10314

Received March 31, 2006; Revised Manuscript Received July 6, 2006

ABSTRACT: Minibrain kinase/dual-specificity tyrosine phosphorylation regulated kinase 1A (MNB/DYRK1A) is a proline/arginine-directed serine/threonine kinase implicated in the learning deficits of Down syndrome. Epigallocatechin-3-gallate (EGCG), the major tea polyphenolic compound, is a potent MNB/DYRK1A inhibitor. In this study, we investigated the mechanism of EGCG inhibition of MNB/DYRK1A using a combination of genetic and biochemical approaches. In the testing system using MNB/DYRK1A-promoted Gli 1-dependent transcription as the readout, NIH3T3 cells expressing EGCG resistant MNB/DYRK1A mutant R21 were found to acquire EGCG resistance for a wide range of drug concentrations. Mutant R21 harbors a single K465R substitution, which produces a 3-fold gain in the EGCG resistance in vitro. However, the gain in the EGCG resistance alone cannot fully interpret the effectiveness of mutant R21 in suppressing EGCG in cultured cells. Kinetic analysis suggests that EGCG functions as a noncompetitive inhibitor against ATP. Interestingly, the K465R mutation changes the mode of EGCG inhibition on MNB/DYRK1A so that it becomes a competitive inhibitor against ATP. This competitive mode of EGCG inhibition coupled with high intracellular ATP concentrations and an elevated EGCG resistance are likely to be the basis for the resistant property of mutant R21 in cultured cells. The K465R mutation apparently transforms the intramolecular interactions required for MNB/DYRK1A catalysis. This mutant would also be valuable for the elucidation of the mechanisms of MNB/DYRK1A-catalyzed reaction.

Minibrain kinase (MNB) was first discovered in *Drosophila* as an essential factor involved in post-embryonic neurogenesis (*1*). The homologue of *Drosophila* MNB, dual-specificity tyrosine phosphorylation-regulated kinase 1A (DYRK1A), is highly conserved among different organisms (*2*−*4*). Despite the name of dual-specificity, MNB/DYRK1A[1] functions as a proline/arginine-directed serine/threonine kinase toward exogenous substrates (*5*−*11*). This kinase is a member of the DYRK family, which in turn belongs to the CMGC group of protein kinases (*2*, *12*).

In addition to the conserved kinase subdomains (residues 160−480 for MNB/DYRK1A) shared by all kinases, the DYRK family possesses a number of family-specific characteristic motifs in the kinase subdomains. These motifs include the sequence SSC following the conserved motif ^{307}DFG^{309} in subdomain VII, a replacement of the conserved arginine in subdomain VIB by cysteine, and the ^{319}YXY^{321} motif between subdomains VII and VIII (*2*, *13*). The YXY motif of MNB/DYRK1A has been postulated to be the equivalent of the TXY motif (phosphorylation lip) of ERK (*14*, *15*). ERK activation requires the phosphorylation of both threonine and tyrosine residues in this motif by the upstream kinase (*16*, *17*). Active MNB/DYRK1A (expressed either in *Escherichia coli* or other systems) contains phosphotyrosine (PY) in the YXY motif (*15*, *18*), and MNB/DYRK1A harboring the tyrosine to phenylalanine substitution in the YXY motif has a drastically reduced PY content and kinase activity (*15*, *18*). These observations suggest that tyrosine phosphorylation (through autophosphorylation) in the YXY motif is necessary for MNB/DYRK1A activity (*18*). Interestingly, for members of the DYRK family, tyrosine autophosphorylation can only occur during protein synthesis but not in the matured protein. Thus, tyrosine autophosphorylation has been postulated to be a "one-off" inceptive event for kinase activation (*19*).

The MNB/DYRK1A gene is located in the Down syndrome (DS) critical region of human chromosome 21 (*20*−*24*), and its expression is apparently elevated in DS patients (*25*−*27*). Animal studies with MNB/DYRK1A transgenic mice further demonstrate a correlation between MNB/DYRK1A overexpression and developmental delay (*28*−*30*). Together, the evidence suggests that MNB/DYRK1A overexpression may be an etiological basis for certain DS phenotypes.

† This work is supported in part by the New York State Office of Mental Retardation and Developmental Disabilities and by NIH Grants HD38295 (Y.W.H.) and HD43960 (J.W.).

* To whom correspondence should be addressed: Yu-Wen Hwang, Molecular Biology Department, NYS Institute for Basic Research in Developmental Disabilities, 1050 Forest Hill Road, Staten Island, NY 10314. Tel: 718-494-5337. Fax: 718-494-5905. E-mail: hwang@mail.csi.cuny.edu.

‡ Molecular Biology Department.

§ Develomental Neurobiology Department.

[1] Abbreviations: DMEM, Dulbecco's modified Eagle's medium; DS, Down syndrome; D3, dynatide 3; EGCG, (−)-epigallocatechin-3-gallate; ERK, extracellular signal-regulated protein kinase; GST, glutathione-S-transferase; IPTG, isopropyl-*β*-D-thiogalactopyranoside; MNB/DYRK1A, minibrain kinase/dual-specificity tyrosine phosphorylation-regulated kinase 1A; WT, wild-type.

10.1021/bi060632j CCC: $33.50
Published on Web 09/07/2006

We have been searching for a specific means by which to perturb MNB/DYRK1A. Several compounds have been shown to inhibit MNB/DYRK1A. These chemicals include epigallocatechin-3-gallate (EGCG), purvalanol, roscovitine, 4,5,6,7-tetrabromobenzotriazole, and others (*31*−*34*). In the surveys conducted with 30+ kinases and numerous inhibitors, EGCG emerged as the most effective (and specific) MNB/DYRK1A inhibitor (*31*, *32*). However, EGCG, in sufficiently high concentrations, is known to disrupt many enzymes and cellular processes (*31*, *35*−*38*). This complexity makes it unsuitable for using EGCG alone as a tool to investigate the function of MNB/DYRK1A in any complex cellular system. Despite this limitation, the elucidation of the mechanism of EGCG inhibition may provide helpful insight into designing a specific means by which to inhibit MNB/DYRK1A. In this report, we describe the properties of a MNB/DYRK1A mutant that confers EGCG resistance in cultured cells by changing the kinetic mode of inhibition.

MATERIALS AND METHODS

Clone Construction. The GST fusion full-length clone (pGEX-Mnb) was described previously (*39*). The truncated (at residue 497) MNB/DYRK1A mutant was produced by PCR using the following oligonucleotides: tctcatcgatgcatacaggaggagacttcag and cctctcgagctaacggtccatccactttc as the 5′ and 3′ primers, respectively. A termination codon was introduced at residue 498 of MNB/DYRK1A by the 3′ primer. The amplicon was then cloned into the Cla I and Xho I sites of a modified pGEX vector as described (*39*). To construct the R21 mammalian expression vector, mutant R21 was first restored to full-length in the pRHC-Mnb type clone (*10*) by utilizing the unique Cla I (partially overlaps with the start codon) and Pst I (located at around codon 476 of MNB/DYRK1A) sites in these plasmids. This step replaces the last 21 amino acids of truncated R21 (containing no mutation) with the WT sequence from residue 476 to the C-terminus. The MNB/DYRK1A gene in the resulting pRHC-Mnb(R21) was then spliced into the pCMV-Script vector (Stratagene) through the Hind III and Xho I sites to produce pCMV-Mnb vectors. The mammalian vector for expressing human Gli 1 gene, pcGli1, was constructed by inserting the Hind III-Xho I Gli fragment from GLIK12 (*40*) into the corresponding sites of the pcDNA3 vector. GST fusion truncated MNB/DYRK1A containing the K465R substitution was constructed by the QuikChange site-directed mutagenesis system obtained from Stratagene.

Protein Purification. All GST fusion proteins were expressed in *E. coli* strain BL21 by incubating cell culture (at OD about 1) with 0.5 mM IPTG for 16 h at 20 °C. The full-length and truncated forms of GST-MNB/DYRK1A were first purified by glutathione resin, as previously described (*39*). Proteins were further purified by a batch method using Q Sepharose resin. Briefly, GST fusion proteins (diluted in 25 mM Tris-HCl, pH 7.4) were adsorbed to Q Sepharose resin, washed extensively with a buffer containing 25 mM Tris-HCl (pH 7.4) and 100 mM NaCl, and then eluted with the same buffer containing 200 mM NaCl.

Kinetic Analysis and EGCG Inhibition Assay. Kinetic measurements were performed in a total volume of 30 μL solution consisting of 1× kinase buffer (25 mM HEPES, 100 mM NaCl, and 5 mM $MgCl_2$), 10−100 μM ATP, 2 μCi [γ-^{32}P]-ATP, 12−96 μM dynatide 3 (D3), 50 ng kinase, and EGCG if needed. The amounts of EGCG used were 0.2−0.6 μM for wild-type (WT) and 0.6−2.4 μM for mutant R21. EGCG (cat. no. E4143) was purchased from Sigma and used without further purification. Reactions were initiated by the addition of kinase and were allowed to proceed for 10 min at 30 °C. Under these conditions, less than 10% of D3 was phosphorylated. At the end of the incubation, a 5 μL aliquot of the reaction mixture was withdrawn and spotted on a P81 membrane. The partially dried membranes were washed 4 times (each for 5 min) with large excess of 0.1 M phosphoric acid and once with 95% ethanol as described (*10*). The radioactivity retained on membrane was then measured in a scintillation counter, corrected for the backgrounds, and then used for calculating the reaction rate. The data used for plotting and calculation represent the average of at least three independent experiments. The kinetic parameters for the two-substrate kinetics were determined by fitting the data iteratively to the equation $v = V_{max}[S_A][S_B]/(K_{AB} + K_{mB}[S_A] + K_{mA}[S_B] + [S_A][S_B])$ using program Leonora (*41*). K_{cat} was subsequently calculated as V_{max}/[MNB/DYRK1A]. The K_I for the competitive and the noncompetitive modes of EGCG inhibition were similarly calculated by fitting the data to the equation $v = V_{max}[S]/(K_m(1 + [EGCG]/K_I) + [S])$ and the equation $v = V_{max}[S]/(K_m(1 + [EGCG]/K_I) + [S](1 + [EGCG]/K_I))$, respectively.

EGCG sensitivity assay was performed in a 30 μL reaction mixture similarly as described above, except with twice the original amount of kinase. Seven concentrations of EGCG ranging from 0.05 to 6.4 μM were used for each determination. Reactions were initiated by the addition of kinase and allowed to proceed for 20 min at 30 °C. D3 phosphorylation was then determined by the P81 membrane binding assay as described above and used as a parameter for kinase activity. The activity of MNB/DYRK1A in the presence of a given EGCG concentration was calculated as the percent of activity to the control containing no EGCG and then plotted against log [EGCG]. The approximate EGCG concentration for 50% inhibition of MNB/DYRK1A was subsequently estimated from the plots. The data presented in Table 1 were the average of at least two independent trials.

Table 1: EGCG Sensitivity and Mutation Sites of EGCG Resistant Mutants[a]

mutant	apparent IC_{50} (μM)	mutation sites
WT (full length)	0.42 ± 0.06	not applicable
WT	0.43 ± 0.05	not applicable
R20	0.70 ± 0.09	D143E; L224M; P380T
R21	1.41 ± 0.12	K465R
R34	0.95 ± 0.16	W403R; Y415F; L457I
R53	0.74 ± 0.11	A33E; I101V; I303F; V306A; A364D

[a] All MNB/DYRK1As used for analysis were truncated proteins except indicated otherwise.

EGCG Resistant Mutants Isolation. Random mutagenesis was performed using the PCR-based GeneMorph II random mutagenesis kit obtained from Stratagene. The full-length pGEX-Mnb (*39*) was used as the template, and the oligonucleotides pairs used for constructing truncated MNB/DYRK1A mutant at residue 497 (see above) were used as

Table 2: Kinetic Parameters for WT and R21 MNB/DYRK1A

	K_m (μM)		K_{cat} (min^{-1})	K_I (μM) EGCG	
	ATP	D3		ATP[a]	D3[b]
WT	55.21 ± 10.43	70.72 ± 13.02	20.36 ± 2.69	0.33 ± 0.04	0.41 ± 0.08
R21	57.08 ± 9.79	65.86 ± 11.51	14.73 ± 2.16	1.03 ± 0.09	1.25 ± 0.17

[a] Performed with 24 μM D3. [b] Performed with 50 μM ATP.

the primers for PCR. The protocol was adjusted to produce no more than 4∼5 misincorporations per kilobase of target DNA. The resulting amplicon (about 1500 bp containing codon 1−497) was digested with Cla I and Xho I and then recloned into the pGEX vector to create a mutant pool. The initial pool contained about 180 independent mutants. For mutant screening, each individual candidate was first cultured overnight (without shaking), diluted (in 1 mL total), and induced for MNB/DYRK1A synthesis with 0.5 mM IPTG for 4 h at 37 °C. A crude MNB/DYRK1A preparation was obtained by resuspending the cell pellets from 1 mL culture in 0.1 mL of B-Per (Pierce Chemical Co.) for 10 min at room temperature followed by centrifugation at 12000*g* for 5 min. The kinase reaction was performed in a 50 μL mixture consisting of 1× kinase buffer, 10 μL of crude lysate, 50 μM ATP, 1 μg of dynatide 3, 2 μCi of [γ-^{32}P]-ATP, and either with or without 20 μM EGCG. The reactions were allowed to proceed for 20 min at 30 °C. The phosphorylation of dynatide 3 was measured as described above. A parallel experiment with cells harboring the wild-type (WT) construct was conducted in the group for comparison. A total of 92 out of the original pool of 180 clones were screened.

Gli 1-Dependent Transcription Assay. The assay was performed similarly as described by others (*42*). Briefly, NIH3T3 cells were seeded in DMEM plus 10% calf serum at a density of 4×10^5 cells per well in a 24-well plate and used immediately for transfection using the Lipofectamine 2000 reagent (Invitrogen). Vectors pcGLI (Gli1 expression vector) and 3′ 8xGli-BS-Luc (luciferase reporter vector) (*43*) at 0.1 μg each were cotransfected with 0.3 μg of pCMV-Mnb (either WT or mutant R21) and 0.01 μg of pRL-TK (Renilla luciferase internal transfection control vector for dual-luciferase reporter assay, obtained from Promega) for 5 h at 37 °C. Gene expression was then allowed to continue for an additional 24 h and quantified using dual-luciferase reporter assay system (Promega). Luciferase activity was recorded with a manual Turner Designs luminometer TD20/20 set for dual-luciferase reading, where the (second) reading of Renilla luciferase activity was used as the internal control. The ratio of the two recordings was used for data analysis. When needed, transfected cells were treated with the indicated amounts of EGCG at the end of transfection and processed for luciferase assay as described above. For monitoring the level of MNB/DYRK1A expression, 10 μg of cell lysate prepared for the luciferase assay were probed with anti-MNB/DYRK1A mAb 7F3 in immunoblotting as previously described (*44*).

RESULTS

Isolation of EGCG Resistant Mutants. EGCG was reported to inhibit MNB/DYRK1A with an IC_{50} of 0.33 μM (at 100 μM ATP) (*31*). We have obtained similar results for both *E. coli*-expressed GST fusion full-length and truncated (residues 1−497) MNB/DYRK1A by using dynatide 3 (D3) as the substrate (*10*) (Table 1). The truncated MNB/DYRK1A contains the entire kinase domain (residues 160−480) plus an additional 160 residues to its N-terminal end. This truncation is known to possess the kinetic activity of the intact protein (*15*), which we subsequently confirmed (see Table 2 for truncated MNB/DYRK1A and ref *10* for the full-length protein). The inhibition data indicate that the last 266 residues of MNB/DYRK1A are not required for interacting with EGCG (Table 1). Thus, the truncated MNB/DYRK1A was used as the template for isolating EGCG resistant mutants.

Since there was no known method for selecting EGCG resistant mutants, we screened mutants by a direct kinase assay. To expedite the process, an assay for testing EGCG sensitivity in crude cell lysate was developed. The use of crude cell lysate reduces the time for sample preparation. Briefly, we induced the expression of truncated GST fusion MNB/DYRK1A using IPTG in *E. coli*, which we then followed with cell lysis in the B-PER reagent. The crude lysate was then used as the source of kinase to phosphorylate D3. As shown in Figure 1A, the IPTG-induced cells clearly produced sufficient kinase to distinguish them from the uninduced background (column 1 vs column 2). Most importantly, the induced activity was inhibited by 20 μM of EGCG (column 2 vs column 4). To generate measurable inhibition in crude *E. coli* lysate, however, EGCG at concentrations much higher than the IC_{50} (Table 1) must be used.

Mutants were screened individually via the EGCG assay as described in Figure 1 from a pool of random mutants constructed on GST fusion truncated MNB/DYRK1A. Any mutant with an EGCG resistance (the ratio of with EGCG vs without EGCG shown as the relative activity in Figure 1) of at least twice that of the wild-type (WT) was purified for further analysis (Figure 1B). Four mutants out of 92 screened were further analyzed and found to gain moderately in EGCG resistance (Table 1). The mutation sites in all four resistant mutants were mapped, and all but mutant R21 contained multiple amino acid substitutions (Table 1). Interestingly, most of the mutation sites were localized in the regions of MNB/DYRK1A corresponding to kinase subdomains X and XI (*2*, *12*). These subdomains are away from the ATP binding and the catalytic sites (*45*−*49*). Mutant R21 harbors two base substitutions, one of which leads to the Lys to Arg mutation at residue 465 of MNB/DYRK1A. Mutant R21 was selected for further study because it contains WT-like catalytic activity (see below), the highest EGCG resistance, and only a single amino acid substitution.

Property of Mutant R21 in Cultured Cells. MNB/DYRK1A has been shown to positively regulate Gli 1-dependent transcription (*42*). Thus, the system was utilized to measure the property of the R21 mutant in culture cells. The basic assay consists of cotransfecting host cells with a mixture of a Gli 1 expression vector (*40*) and a luciferase reporter vector containing Gli 1 binding sequence (*43*). To perform the cell culture assay, both WT and mutant R21 were first restored to the full-length construct (Materials and Methods) in the mammalian expression vector pCMV-Script. The luciferase output of this system could be drastically elevated if MNB/DYRK1A is included in the cotransfection (*42*). In NIH 3T3 cells, the inclusion of the WT MNB/

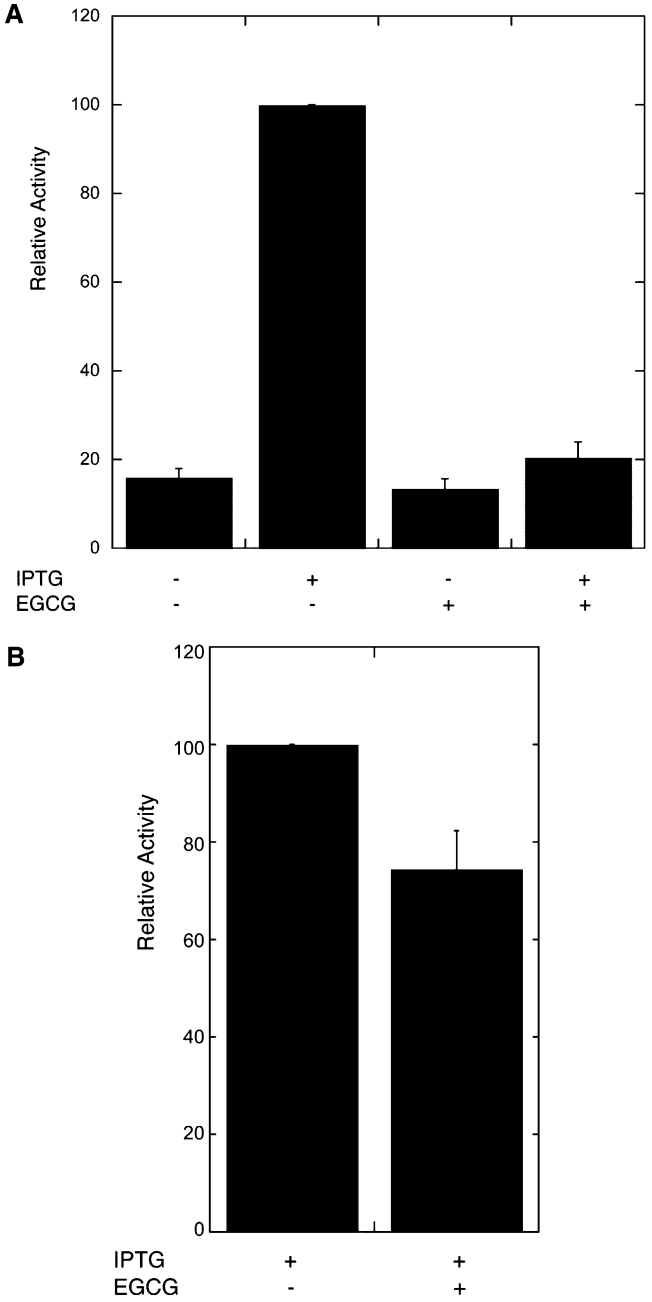

FIGURE 1: Inhibition of truncated MNB/DYRK1A by EGCG in crude lysate. Crude lysate was prepared from IPTG-induced (IPTG +) and uninduced (IPTG −) *E. coli* strain BL21 harboring the truncated MNB/DYRK1A vector as described in the Materials and Methods. The crude lysate was then subjected to kinase assay by measuring D3 phosphorylation in the presence (+) or absence (−) of 20 μM EGCG. The data were the average from two independent trials and were normalized to the samples of the IPTG-induced control (without EGCG) before plotting. (A) WT. (B) mutant R21.

DYRK1A vector, pCMV-Mnb(WT), in the cotransfection enhanced the luciferase output to about 6 times that of the vector control (pCMV) (Figure 2A). Under the same experimental conditions, mutant R21 was found to display about 75% of WT's activity (Figure 2A) while the expression level was comparable to that of WT (Figure 2B).

We then examined whether the expression of exogenous mutant R21 could confer EGCG resistance to the recipient cells in the same Gli 1-dependent transcription system. The experiments were performed similarly as described in Figure 2, except that the transfected cells were exposed to EGCG

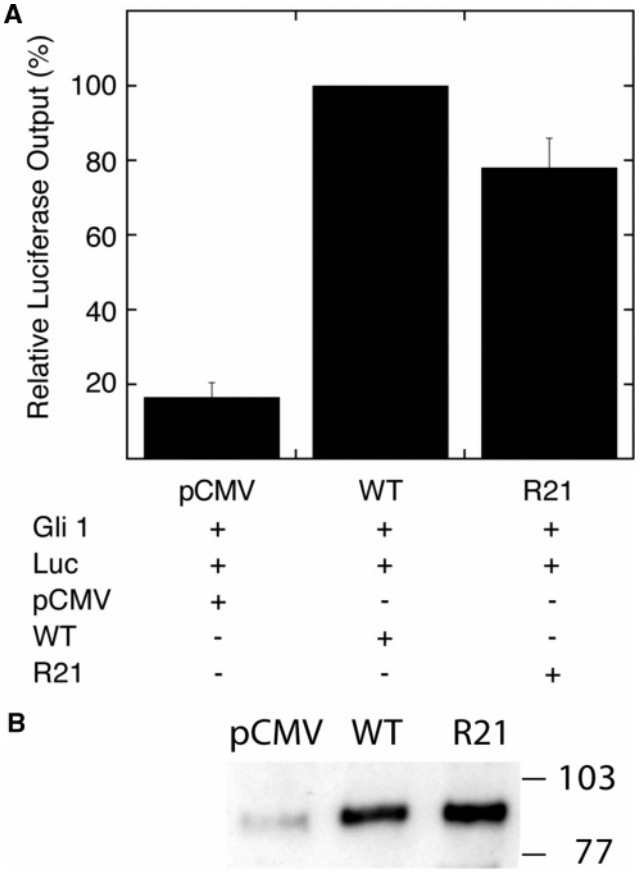

FIGURE 2: Activity and expression of the full-length mutant R21 in NIH3T3 cells. (A) MNB/DYRK1A activity in cultured cells. The activity was measured by the Gli 1-dependent luciferase assay. Briefly, NIH 3T3 cells were transfected with pcGLI (Gli1), 3′Gli-BS-Luc (Luc), and pRL-TK (renilla luciferase internal transfection control vector) plasmids together with either pCMV, pCMV-Mnb-(WT), or pCMV-Mnb(R21) for 24 h and analyzed as described in the Materials and Methods. The full-length MNB/DYRK1A constructs were used for all analysis in cultured cells. After correcting for the internal control, the luciferase output was normalized to the reactions promoted by pCMV-Mnb(WT) (=100%) before plotting. The data represent the average of three independent trials. (B) Expression of WT and mutant R21 in transfected cells. The level of MNB/DYRK1A was detected by immunoblotting using anti-MNB/DYRK1A antibody mAb 7F3 (*44*) on the same samples prepared for luciferase assay. A typical result was shown.

during the 24 h incubation period prior to the luciferase assay. The presence of EGCG (25−100 μM) caused a concentration-dependent inhibition of lucifrase output promoted by WT MNB/DYRK1A (Figure 3). The EGCG concentration required for inhibiting MNB/DYRK1A activity (luciferase output) in cultured cells is much higher than that in vitro. This may be because the effective concentration of EGCG is reduced by various cellular components. Furthermore, EGCG is known to metabolize readily under cell culture conditions (*50*). In contrast to the WT-driven expression, EGCG exhibited no apparent inhibitory effect when the Gli 1-dependent transcription activity was promoted by mutant R21 (Figure 3). In fact, a small but consistent increase in Gli 1-dependent output was observed in R21 transfected cells for concentrations of up to 100 μM EGCG. Under our assay conditions, EGCG produced no visible growth retardation on NIH 3T3 cells until its concentration reached about 200−250 μM (measured after 24 h of treatment). At these EGCG concentrations, both the cell viability and the Gli 1-dependent

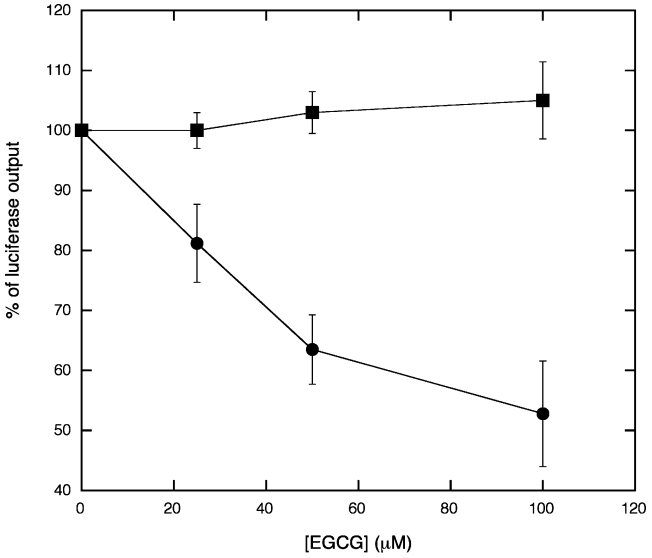

FIGURE 3: EGCG sensitivity of Gli 1-dependent transcription. The assays were performed similarly as described in Figure 2 except that transfected cells were treated with EGCG (0−100 μM) at the end of transfection and continued for 24 h. The luciferase output from the transfected cells treated with EGCG was normalized to that of each respective untreated control (set at 100% for both WT and R21) before plotting. Figure 2A shows the typical results for the starting point of normalization. Gli 1-transcription promoted by WT (●) and mutant R21 (■) MNB/DYRK1A. The average from three independent trials was presented.

transcription were severely reduced regardless of whether WT or R21 was expressed in these cells (data not shown)

Kinetic Analysis of Mutant R21. With only a moderate gain in EGCG resistance, the effectiveness of suppressing EGCG by mutant R21 in cultured cells is surprising. Therefore, we sought a possible kinetic explanation for this property of mutant R21 in cultured cells. All the kinetic assays were performed with truncated proteins because the quality of protein preparation is consistently much better for the truncated protein than for the full-length MNB/DYRK1A. This may be due to the removal of a PEST sequence from the C-terminal domain of MNB/DYRK1A by truncation.

MNB/DYRK1A uses both ATP and D3 as substrates. First, we examined whether the kinetics of MNB/DYRK1A follow the sequential or the ping-pong mechanism (*51*). Double-reciprocal plots of initial rate data obtained with varied [ATP] and several constant [D3] produced a set of lines intersecting to the left of the *y*-axis (Figure 4A). Similar results were obtained when experiments were performed with varied [D3] and constant [ATP] (Figure 4B). These results suggest that MNB/DYRK1A catalysis follows the sequential kinetic mechanism by forming ternary kinase-ATP-D3 complexes rather than by the ping-pong mechanism (*51*). The kinetic parameters for these two substrates were subsequently determined to be 55.21 ± 10.43 μM, 70.72 ± 13.02 μM, and 20.36 ± 2.69 min^{-1} for K_m(ATP), K_m(D3), and K_{cat}, respectively (Table 2). We then determined the kinetics of EGCG inhibition. EGCG inhibition experiments with a constant [D3] (24 μM) and varied [ATP] produced a set of lines intersecting at the *x*-axis in the double-reciprocal plot (Figure 5A). Similarly, experiments performed with a constant [ATP] (50 μM) and varied [D3] also generated a set of lines intersecting at the *x*-axis (Figure 5B). These results suggest that EGCG functions as a noncompetitive inhibitor against either ATP

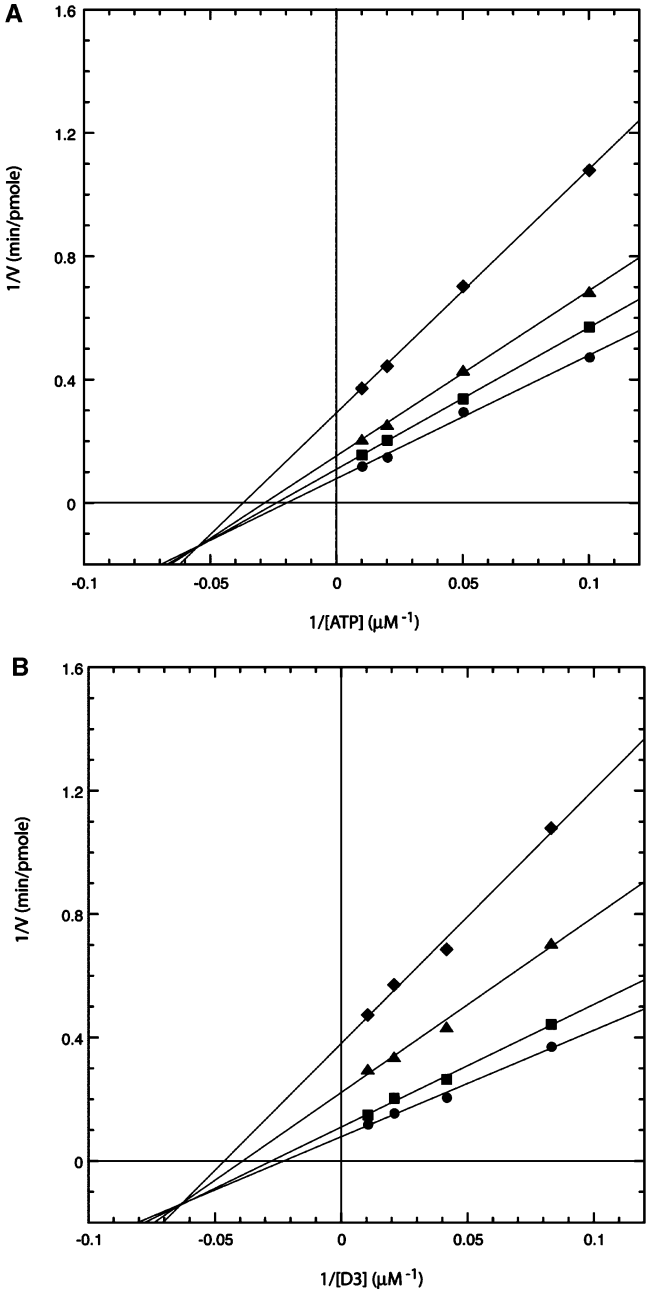

FIGURE 4: Two-substrate kinetic profile of the phosphorylation reaction catalyzed by truncated MNB/DYRK1A. (A) Effects of increasing D3 concentrations on reaction rate. The reaction was performed with varied ATP concentrations (10−100 μM) at four constant D3 concentrations (12−96 μM) as described in the Materials and Methods. The initial rates and ATP concentration were then plotted as 1/*V* vs 1/[ATP]. D3 concentrations used in the reaction: (◆) 12 μM, (▲) 24 μM, (■) 48 μM, (●) 96 μM. (B) Effects of increasing ATP concentrations on reaction rate. The data obtained in Figure 1A was rearranged and replotted as 1/*V* vs 1/[D3]. ATP concentrations used in the reactions: (◆) 10 μM, (▲) 20 μM, (■) 50 μM, (●) 100 μM.

or D3. The kinetic mechanism of EGCG inhibition is consistent with the finding that most EGCG resistance mutations are mapped at sites distal to the substrate binding sites (Table 1). The K_Is for the ATP and D3 competition assays were subsequently determined to be 0.33 ± 0.04 μM and 0.41 ± 0.08 μM, respectively (Table 2).

Analysis of mutant R21 revealed that the K465R mutation did not significantly alter MNB/DYRK1A's kinetic

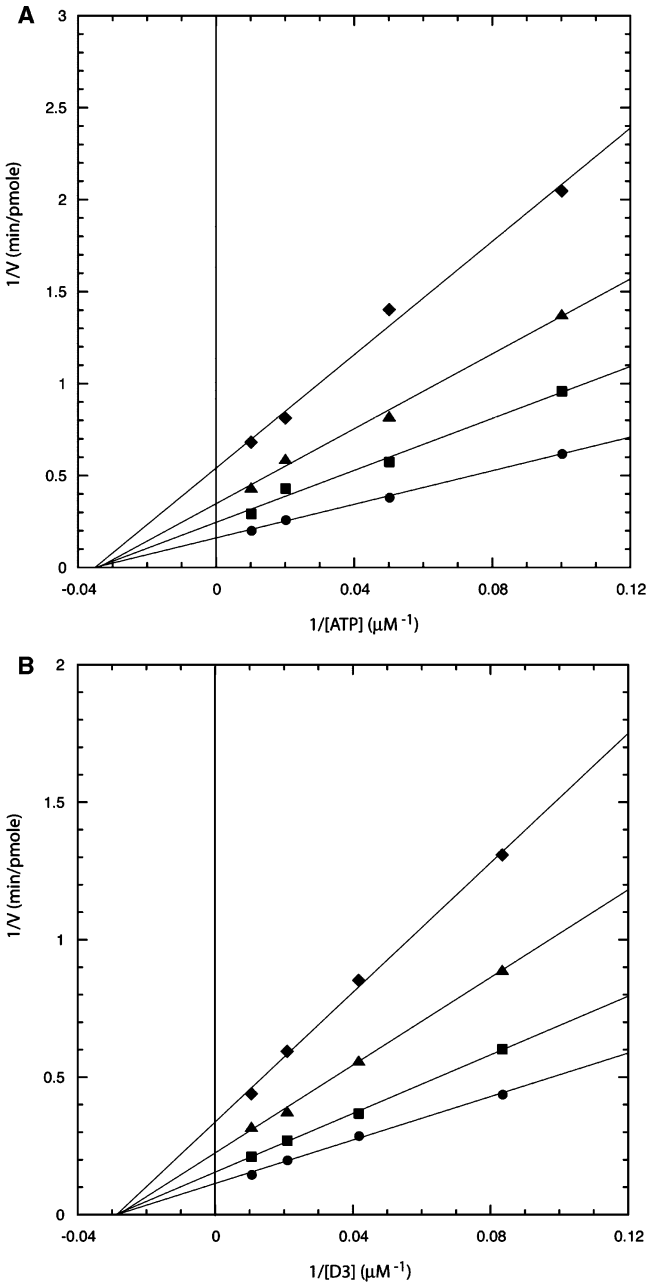

FIGURE 5: Inhibition of truncated WT MNB/DYRK1A by EGCG. (A) Competition of EGCG against ATP. The reaction was performed with varied ATP concentrations (10−100 μM) at four constant EGCG concentrations (0−0.8 μM) as described in the Materials and Methods. D3 at a constant concentration (24 μM) was used for all reactions. The initial rates and ATP concentration were then plotted as 1/*V* vs 1/[ATP]. (B) Competition of EGCG against D3. The reaction was performed with varied D3 concentrations (12−96 μM) at four constant EGCG concentrations (0−0.8 μM) similarly as described above. ATP at a constant concentration (50 μM) was used for all reactions. The initial rates and ATP concentration were then plotted as 1/*V* vs 1/[D3]. EGCG concentrations used in the reactions: (●) 0, (■) 0.2 μM, (▲) 0.4 μM, (◆) 0.8 μM.

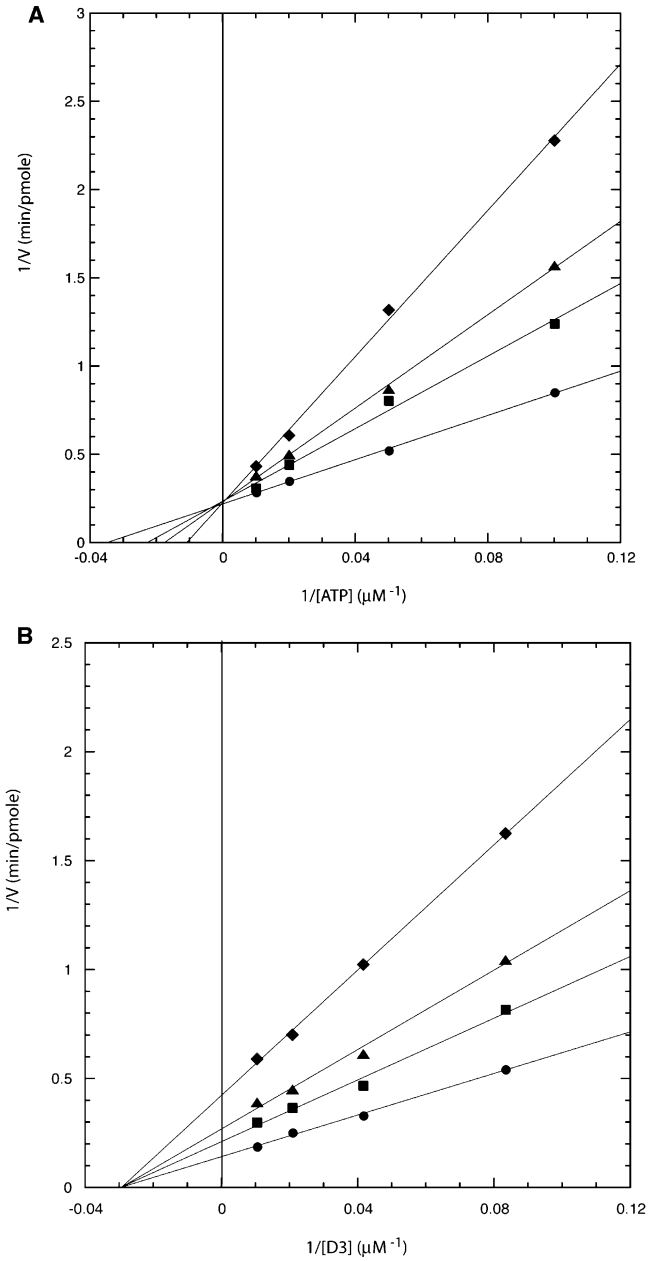

FIGURE 6: Inhibition of truncated MNB/DYRK1A mutant R21 by EGCG. (A) Competition of EGCG against ATP. The reaction was performed exactly as described in Figure 5 except with different EGCG concentrations. (B) Competition of EGCG against D3. The reaction was performed exactly as described in Figure 1B except with different EGCG concentrations. EGCG concentrations used in the experiments: (●) 0, (■) 0.6 μM, (▲) 1.2 μM, (◆) 2.4 μM.

properties. The K_m for ATP and D3 was basically unchanged while the K_{cat} for D3 was only moderately reduced (Table 2). The K465 residue, which is localized near the highly conserved Arg residue (R467 in MNB/DYRK1A) in kinase subdomain XI, is apparently not directly involved in catalysis. This result is in parallel with the activity of mutant R21 measured in cultured cells (Figure 2A). We subsequently determined the kinetic mechanism of EGCG inhibition for mutant R21 by using the protocol described in Figure 5. Interestingly, EGCG inhibition experiments with a constant [D3] (24 μM) and varied [ATP] produced a set of lines intersecting at (or very close to) the *y*-axis in the double-reciprocal plot (Figure 6A). The pattern of inhibition is consistent with EGCG as a competitive inhibitor against ATP. On the other hand, experiments performed with a constant [ATP] (50 μM) and varied [D3] produced a pattern of inhibition (Figure 6B) similar to that of the WT (Figure 5B). These observations indicate that the K465R mutation changes the mode of EGCG inhibition with ATP but not with D3. The K_Is for the ATP and D3 competition assays were subsequently determined to be 1.03 ± 0.09 μM and

1.25 ± 0.17 μM, respectively (Table 2). The change in EGCG inhibition from a noncompetitive mode to a competitive mode against ATP offers a reasonable explanation for the increased suppression of EGCG found in mutant R21 in NIH 3T3 cells (see Discussion).

DISCUSSION

EGCG, the major tea polyphenolic compound (*52*), is a potent MNB/DYRK1A inhibitor (*31*). To help to understand the effects of EGCG on MNB/DYRK1A, we have investigated the mechanism of EGCG inhibition using a combination of genetic and biochemical approaches.

Accordingly, we have isolated several MNB/DYRK1A mutants resistant to EGCG (Table 1). Mutant R21 was pursued because it has the highest EGCG resistance (Table 1) and a catalytic activity similar to WT in vitro (Table 2). Mutant R21 contains a single K465R mutation (Table 1), and this mutation largely preserves the kinetic properties of MNB/DYRK1A in vitro (Table 2). Consistent with the activity in vitro, mutant R21 was also shown to display comparable enzymatic activity in NIH3T3 cells in enhancing Gli 1-dependent transcription (Figure 2A). Using the same assay system, we further showed that the output of the Gli 1-dependent system is sensitive to EGCG treatment if it was promoted by WT MNB/DYRK1A, but not if it was promoted by mutant R21 (Figure 3). This result confirms that mutant R21 is capable of conferring EGCG resistance to the recipient cells. If MNB/DYRK1A were not previously known to regulate the Gli 1-dependent transcription system, the results shown in Figure 3 would have inferred the involvement of MNB/DYRK1A in this particular system. A similar approach, using drug resistant p38MAPK, has been applied successfully to validate the specificity of SB 203580 in vivo (*53*). Since mutant R21 confers a dominant trait, it is conceivable that the combination of mutant R21 with EGCG could have general applicability. However, in light of the pharmacological complexity of EGCG, the results obtained by the mutant plus EGCG approach would need to be carefully interpreted.

With its moderate gain in EGCG resistance (about 3-fold), mutant R21 was a surprisingly potent suppressor of EGCG in cultured cells (Figure 3). This property of mutant R21 in cultured cells is apparently disconnected from that of mutant R21 in vitro. A solution to this dilemma was offered by the kinetic properties of mutant R21. Steady-state kinetic analysis suggests that EGCG functions as a noncompetitive inhibitor against both ATP and D3 (Figure 5). Although the K465R mutation confers only a small change in EGCG resistance (Tables 1 and 2) to MNB/DYRK1A, it appears to fundamentally alter the intramolecular interactions of MNB/DYRK1A. This is clear from the finding that EGCG becomes a competitive inhibitor against ATP in mutant R21. The intracellular ATP concentration is known to be in mM range (*54*). By coupling an elevated EGCG resistance with high ATP concentrations and the competitive mode of inhibition (EGCG vs ATP), mutant R21 would be expected to maintain normal (or near normal) activity in vivo for far higher EGCG concentrations than the WT. This is likely to be the basis for the effective suppression of EGCG by mutant R21 in vivo. A small change in IC_{50} can also be found in many Bcr-Abl mutants that are resistant to clinical concentrations of STI-571, an ATP competitive inhibitor (*55*).

The catalysis of MNB/DYRK1A goes through a ternary complex (the sequential two-substrate kinetics) consisting of MNB/DYRK1A and both substrates (Figure 4). With its mode of noncompetitive inhibition against both substrates, it suggests that EGCG inactivates MNB/DYRK1A by binding to a distinct site on MNB/DYRK1A, which prevents the ternary complex from completing the catalytic cycle. The existence of a distinct EGCG binding site as suggested by kinetic analysis is consistent with the findings of the mutagenesis study. The majority of the mutations identified in EGCG resistant mutants are located in kinase subdomain X and beyond. In fact, the two mutants (R21 and R34) with the most EGCG resistance contain exclusively mutations located in either subdomains X or XI. Although the crystal structures of MNB/DYRK1A are not yet available, kinase subdomains X and XI are located distal to the ATP binding site and the catalytic pocket in many kinases with known structures (*45*−*49*). The comparison is especially significant between MNB/DYRK1A and ERK2 because these two proteins share considerable homologues in the kinase domain (*2*, *12*). Therefore, we postulate that EGCG binds to a site in/around kinase subdomain X−XI and inhibits the catalysis of MNB/DYRK1A. The ability of the K465R mutation to alter the mode of EGCG inhibition is intriguing. K465 is only a residue away from the highly conserved R467 of MNB/DYRK1A. Although the K465 residue is not directly involved in catalysis, it appears to play an essential accessory role for the kinase reaction as a mutation at this residue alters the intramolecular interactions of MNB/DYRK1A. The elucidation of this mutant is likely to yield valuable information for understanding the molecular mechanisms of EGCG inhibition as well as the MNB/DYRK1A-catalyzed phosphorylation.

ACKNOWLEDGMENT

We thank Drs. Bert Vogelstein and Kenneth Kinzler of The John Hopkins University Medical Institutions for providing Gli 1 vector GLIK12 and Dr. Hiroshi Sasaki of the Center for Developmental Biology, RIKEN Kobe, for providing luciferase reporter vector 3′Gli-BS-Luc. We thank Dr. David L Miller for critical reading of this manuscript and many suggestions.

REFERENCES

1. Tejedor, F., Zhu, X. R., Kaltenbach, E., Ackermann, A., Baumann, A., Canal, I., Heisenberg, M., Fischbach, K. F., and Pongs, O. (1995) Minibrain: a new protein kinase family involved in postembryonic neurogenesis in *Drosophila*, *Neuron. 14*, 287−301.
2. Becker, W., and Joost, H. G. (1999) Structural and functional characteristics of Dyrk, a novel subfamily of protein kinases with dual specificity, *Prog. Nucleic. Acid Res. Mol. Biol. 62*, 1−17.
3. Hämmerle, B., Vera-Samper, E., Speicher, S., Arencibia, R., Martínez, S., and Tejedor, F. J. (2002) Mnb/Dyrk1A is transiently expressed and asymmetrically segregated in neural progenitor cells at the transition to neurogenic divisions, *Dev. Biol. 246*, 259−73.
4. Raich, W. B., Moorman, C., Lacefield, C. O., Lehrer, J., Bartsch, D., Plasterk, R. H., Kandel, E. R., and Hobert, O. (2003) Characterization of *Caenorhabditis elegans* Homologs of the Down Syndrome Candidate Gene DYRK1A, *Genetics 163*, 571−80.
5. Himpel, S., Tegge, W., Frank, R., Leder, S., Joost, H. G., and Becker, W. (2000) Specificity determinants of substrate recognition by the protein kinase DYRK1A, *J. Biol. Chem. 275*, 2431−8.

6. Woods, Y. L., Rena, G., Morrice, N., Barthel, A., Becker, W., Guo, S., Unterman, T. G., and Cohen, P. (2001) The kinase DYRK1A phosphorylates the transcription factor FKHR at Ser329 in vitro, a novel in vivo phosphorylation site, *Biochem. J. 355*, 597−607.
7. Woods, Y. L., Cohen, P., Becker, W., Jakes, R., Goedert, M., Wang, X., and Proud, C. G. (2001) The kinase DYRK phosphorylates protein-synthesis initiation factor eIF2Bepsilon at Ser539 and the microtubule-associated protein tau at Thr212: potential role for DYRK as a glycogen synthase kinase 3-priming kinase, *Biochem. J. 355*, 609−615.
8. Campbell, L. E., and Proud, C. G. (2002) Differing substrate specificities of members of the DYRK family of arginine-directed protein kinases, *FEBS Lett. 510*, 31−6.
9. de Graaf, K., Hekerman, P., Spelten, O., Herrmann, A., Packman, L. C., Bussow, K., Muller-Newen, G., and Becker, W. (2004) Characterization of cyclin L2, a novel cyclin with an arginine/serine-rich Domain: phosphorylation by DYRK1A and colocalization with splicing factors, *J. Biol. Chem. 279*, 4612−24.
10. Huang, Y., Chen-Hwang, M. C., Dolios, G., Murakami, N., Padovan, J., Wang, R., and Hwang, Y. W. (2004) Mnbk/Dyrk1A Phosphorylation Regulates the Interaction of Dynamin 1with SH3 Domain-Containing Proteins, *Biochemistry 43*, 10173−10185.
11. Murakami, N., Xie, W., Lu, R. C., Chen-Hwang, M. C., Wieraszko, A., and Hwang, Y. W. (2006) Phosphorylation of amphiphysin 1 by minibrain kinase/dual-specificity tyrosine-phosphorylation-regulated kinase 1A, a kinase implicated in Down syndrome, *J. Biol. Chem. 281*, 23712−23724.
12. Hanks, S. K., and Quinn, A. M. (1991) Protein kinase catalytic domain sequence database: identification of conserved features of primary structure and classification of family members, *Methods Enzymol. 200*, 38−62.
13. Kannan, N., and Neuwald, A. F. (2004) Evolutionary constraints associated with functional specificity of the CMGC protein kinases MAPK, CDK, GSK, SRPK, DYRK, and CK2alpha, *Protein Sci. 13*, 2059−77.
14. Miyata, Y., and Nishida, E. (1999) Distantly related cousins of MAP kinase: biochemical properties and possible physiological functions, *Biochem. Biophys. Res. Commun. 266*, 291−5.
15. Himpel, S., Panzer, P., Eirmbter, K., Czajkowska, H., Sayed, M., Packman, L. C., Blundell, T., Kentrup, H., Grotzinger, J., Joost, H. G., and Becker, W. (2001) Identification of the autophosphorylation sites and characterization of their effects in the protein kinase DYRK1A, *Biochem. J. 359*, 497−505.
16. Payne, D. M., Rossomando, A. J., Martino, P., Erickson, A. K., Her, J. H., Shabanowitz, J., Hunt, D. F., Weber, M. J., and Sturgill, T. W. (1991) Identification of the regulatory phosphorylation sites in pp42/mitogen-activated protein kinase (MAP kinase), *EMBO J. 10*, 885−92.
17. Canagarajah, B. J., Khokhlatchev, A., Cobb, M. H., and Goldsmith, E. J. (1997) Activation mechanism of the MAP kinase ERK2 by dual phosphorylation, *Cell 90*, 859−69.
18. Kentrup, H., Becker, W., Heukelbach, J., Wilmes, A., Schürmann, A., Huppertz, C., Kainulainen, H., and Joost, H. G. (1996) Dyrk, a dual specificity protein kinase with unique structural features whose activity is dependent on tyrosine residues between subdomains VII and VIII, *J. Biol. Chem. 271*, 3488−3495.
19. Lochhead, P. A., Sibbet, G., Morrice, N., and Cleghon, V. (2005) Activation-Loop Autophosphorylation Is Mediated by a Novel Transitional Intermediate Form of DYRKs, *Cell 121*, 925−36.
20. Shindoh, N., Kudoh, J., Maeda, H., Yamaki, A., Minoshima, S., Shimizu, Y., and Shimizu, N. (1996) Cloning of a human homolog of the *Drosophila* minibrain/rat DyrK gene from 'the Down syndrome critical region" of chromosome 21, *Biochem. Biophys. Res. Commun. 225*, 92−99.
21. Song, W. J., Sternberg, L. R., Kasten-Sportès, C., Van Keuren, M. L., Chung, S. H., Slack, A., Miller, D. E., Glover, T. W., Chiang, P. W., Lou, L., and Kurnit, D. M. (1996) Isolation of human and murine homologues of the *Drosophila* minibrain gene: human homologue maps to 21q22.2 in the Down syndrome "critical region", *Genomics 38*, 331−339.
22. Guimerá, J., Pritchard, M., Nadal, M., and Estivill, X. (1997) Minibrain (MNBH) is a single copy gene mapping to human chromosome 21q22.2, *Cytogenet. Cell. Genet. 77*, 182−184.
23. Ohira, M., Seki, N., Nagase, T., Suzuki, E., Nomura, N., Ohara, O., Hattori, M., Sakaki, Y., Eki, T., Murakami, Y., Saito, T., Ichikawa, H., and Ohki, M. (1997) Gene identification in 1.6-Mb region of the Down syndrome region on chromosome 21, *Genome Res. 7*, 47−58.
24. Chen, H., and Antonarakis, S. E. (1997) Localisation of a human homologue of the *Drosophila* mnb and rat Dyrk genes to chromosome 21q22.2, *Hum. Genet. 99*, 262−265.
25. Guimerá, J., Casas, C., Estivill, X., and Pritchard, M. (1999) Human minibrain homologue (MNBH/DYRK1): characterization, alternative splicing, differential tissue expression, and overexpression in Down syndrome, *Genomics 57*, 407−18.
26. Tassone, F., Lucas, R., Slavov, D., Kavsan, V., Crnic, L., and Gardiner, K. (1999) Gene expression relevant to Down syndrome: problems and approaches, *J. Neural. Transm. Suppl. 57*, 179−95.
27. Ferrer, I., Barrachina, M., Puig, B., Martinez de Lagran, M., Marti, E., Avila, J., and Dierssen, M. (2005) Constitutive Dyrk1A is abnormally expressed in Alzheimer disease, Down syndrome, Pick disease, and related transgenic models, *Neurobiol. Dis. 20*, 392−400.
28. Smith, D. J., and Rubin, E. M. (1997) Functional screening and complex traits: human 21q22.2 sequences affecting learning in mice, *Hum. Mol. Genet. 6*, 1729−33.
29. Altafaj, X., Dierssen, M., Baamonde, C., Martí, E., Visa, J., Guimerá, J., Oset, M., González, J. R., Flórez, J., Fillat, C., and Estivill, X. (2001) Neurodevelopmental delay, motor abnormalities and cognitive deficits in transgenic mice overexpressing Dyrk1A (minibrain), a murine model of Down's syndrome, *Hum. Mol. Genet. 10*, 1915−1923.
30. Ahn, K. J., Jeong, H. K., Choi, H. S., Ryoo, S. R., Kim, Y. J., Goo, J. S., Choi, S. Y., Han, J. S., Ha, I., and Song, W. J. (2006) DYRK1A BAC transgenic mice show altered synaptic plasticity with learning and memory defects, *Neurobiol. Dis. 22*, 463−472.
31. Bain, J., McLauchlan, H., Elliott, M., and Cohen, P. (2003) The specificities of protein kinase inhibitors: an update, *Biochem. J. 371*, 199−204.
32. Sarno, S., de Moliner, E., Ruzzene, M., Pagano, M. A., Battistutta, R., Bain, J., Fabbro, D., Schoepfer, J., Elliott, M., Furet, P., Meggio, F., Zanotti, G., and Pinna, L. A. (2003) Biochemical and three-dimensional-structural study of the specific inhibition of protein kinase CK2 by [5-oxo-5,6-dihydroindolo-(1,2-a)quinazolin-7-yl]acetic acid (IQA), *Biochem. J. 374*, 639−46.
33. Gray, N. S., Wodicka, L., Thunnissen, A. M., Norman, T. C., Kwon, S., Espinoza, F. H., Morgan, D. O., Barnes, G., LeClerc, S., Meijer, L., Kim, S. H., Lockhart, D. J., and Schultz, P. G. (1998) Exploiting chemical libraries, structure, and genomics in the search for kinase inhibitors, *Science 281*, 533−8.
34. Kim, N. D., Yoon, J., Kim, J. H., Lee, J. T., Chon, Y. S., Hwang, M. K., Ha, I., and Song, W. J. (2006) Putative therapeutic agents for the learning and memory deficits of people with Down syndrome, *Bioorg. Med. Chem. Lett. 16*, 3772−6.
35. Adhami, V. M., Ahmad, N., and Mukhtar, H. (2003) Molecular targets for green tea in prostate cancer prevention, *J. Nutr. 133*, 2417S−2424S.
36. Lambert, J. D., and Yang, C. S. (2003) Mechanisms of cancer prevention by tea constituents, *J. Nutr. 133*, 3262S−3267S.
37. Mandel, S., Weinreb, O., Amit, T., and Youdim, M. B. (2004) Cell signaling pathways in the neuroprotective actions of the green tea polyphenol (−)-epigallocatechin-3-gallate: implications for neurodegenerative diseases, *J. Neurochem. 88*, 1555−69.
38. Shimizu, M., and Weinstein, I. B. (2005) Modulation of signal transduction by tea catechins and related phytochemicals, *Mutat. Res. 591*, 147−60.
39. Chen-Hwang, M. C., Chen, H. R., Elzinga, M., and Hwang, Y. W. (2002) Dynamin is a minibrain kinase/dual specificity Yak1-related kinase 1A substrate, *J. Biol. Chem. 277*, 17597−17604.
40. Kinzler, K. W., Ruppert, J. M., Bigner, S. H., and Vogelstein, B. (1988) The GLI gene is a member of the Kruppel family of zinc finger proteins, *Nature 332*, 371−374.
41. Cornish-Bowden, A. (1995) *Analysis of Enzyme Kinetic Data*, Oxford University Press.
42. Mao, J., Maye, P., Kogerman, P., Tejedor, F. J., Toftgard, R., Xie, W., Wu, G., and Wu, D. (2002) Regulation of Gli1 Transcriptional Activity in the Nucleus by Dyrk1, *J. Biol. Chem. 277*, 35156−35161.
43. Sasaki, H., Hui, C., Nakafuku, M., and Kondoh, H. (1997) A binding site for Gli proteins is essential for HNF-3beta floor plate enhancer activity in transgenics and can respond to Shh in vitro, *Development 124*, 1313−22.
44. Wegiel, J., Kuchna, I., Nowicki, K., Frackowiak, J., Dowjat, K., Silverman, W. P., Reisberg, B., DeLeon, M., Wisniewski, T., Adayev, T., Chen-Hwang, M. C., and Hwang, Y. W. (2004) Cell

type- and brain structure-specific patterns of distribution of minibrain kinase in human brain, *Brain Res. 1010*, 69−80.
45. Knighton, D. R., Zheng, J. H., Ten Eyck, L. F., Ashford, V. A., Xuong, N. H., Taylor, S. S., and Sowadski, J. M. (1991) Crystal structure of the catalytic subunit of cyclic adenosine monophosphate-dependent protein kinase, *Science 253*, 407−14.
46. De Bondt, H. L., Rosenblatt, J., Jancarik, J., Jones, H. D., Morgan, D. O., and Kim, S. H. (1993) Crystal structure of cyclin-dependent kinase 2, *Nature 363*, 595−602.
47. Zhang, F., Strand, A., Robbins, D., Cobb, M. H., and Goldsmith, E. J. (1994) Atomic structure of the MAP kinase ERK2 at 2.3 A resolution, *Nature 367*, 704−11.
48. Xu, W., Doshi, A., Lei, M., Eck, M. J., and Harrison, S. C. (1999) Crystal structures of c-Src reveal features of its autoinhibitory mechanism, *Mol. Cell 3*, 629−38.
49. Schindler, T., Sicheri, F., Pico, A., Gazit, A., Levitzki, A., and Kuriyan, J. (1999) Crystal structure of Hck in complex with a Src family-selective tyrosine kinase inhibitor, *Mol. Cell 3*, 639−48.
50. Sang, S., Lee, M. J., Hou, Z., Ho, C. T., and Yang, C. S. (2005) Stability of tea polyphenol (−)-epigallocatechin-3-gallate and formation of dimers and epimers under common experimental conditions, *J. Agric. Food Chem. 53*, 9478−9484.
51. Segel, I. (1975) *Enzyme Kinetics, Behavior and Analysis of Rapid Equilibrium and Steady-State Enzyme Systems*, John Wiley & Sons, Inc.
52. Yang, C. S., Maliakal, P., and Meng, X. (2002) Inhibition of carcinogenesis by tea, *Annu. Rev. Pharmacol. Toxicol. 42*, 25−54.
53. Eyers, P. A., van den, I. P., Quinlan, R. A., Goedert, M., and Cohen, P. (1999) Use of a drug-resistant mutant of stress-activated protein kinase 2a/p38 to validate the in vivo specificity of SB 203580, *FEBS Lett. 451*, 191−6.
54. Marcussen, M., and Larsen, P. J. (1996) Cell cycle-dependent regulation of cellular ATP concentration, and depolymerization of the interphase microtubular network induced by elevated cellular ATP concentration in whole fibroblasts, *Cell Motil. Cytoskeleton 35*, 94−99.
55. Azam, M., Latek, R. R., and Daley, G. Q. (2003) Mechanisms of autoinhibition and STI-571/imatinib resistance revealed by mutagenesis of BCR-ABL, *Cell 112*, 831−43.

BI060632J